Journal of Applied Polymer Science

Formation and Characterization of Perfluorocyclobutyl Polymer Thin Films

Jinxiang Zhou,[1] Jianyong Jin,[2*] Adam T. Haldeman,[2] Earl H. Wagener,[2] Scott M. Husson[1]

[1]Department of Chemical and Biomolecular Engineering, Center for Advanced Engineering Fibers and Films, Clemson University, Clemson, South Carolina 29634

[2]Tetramer Technologies LLC, Pendleton, South Carolina 29670

*Present address: School of Chemical Sciences, The University of Auckland, Tamaki Innovation Campus, 261 Morrin Road, St. Johns, Auckland Private Bag 92019, Auckland 1142, New Zealand.

Correspondence to: S. M. Husson (E-mail: shusson@clemson.edu)

ABSTRACT: Perfluorocyclobutyl (PFCB) polymers are a new class of materials that show promise as selective layer materials in the development of composite membranes for gas separations, such as carbon dioxide/methane ($\alpha_{\text{pure gas}} = 38.6$) and oxygen/nitrogen ($\alpha_{\text{pure gas}} = 4.8$) separations. In many of the flat sheet applications, a thin film of the selective layer that is free of major defects must be coated onto a support membrane. A focus of this study was to elucidate the impacts of solvents, polymer concentration, and dip-coating withdrawal speed on PFCB thin film thickness and uniformity. An extension was proposed to the Landau–Levich model to estimate the polymer film thickness. The results show that the extended model fits the thickness-withdrawal speed data well above about 55 mm/min, but, at lower withdrawal speeds, the data deviated from the model. This deviation could be explained by the phenomenon of polymer surface excess. Static surface excesses of polymer solutions were estimated by applying the Gibbs adsorption equation using measured surface tension data. Prepared films were characterized by ellipsometry. Refractive index was found to increase with decreasing film thickness below about 50 nm, indicating densification of ultrathin films prepared from PFCB solutions below the overlap concentration. Atomic force microscopy was used to characterize surface morphologies. Films prepared from tetrahydrofuran and chloroform yielded uniform nanolayers. However, films prepared using acetone as solvent yielded a partial dewetting pattern, which could be explained by a surface depletion layer of pure solvent between the bulk PFCB/acetone solution and the substrate. © 2013 Wiley Periodicals, Inc. J. Appl. Polym. Sci. 129: 3226–3236, 2013

KEYWORDS: surfaces and interfaces; coatings; films; membranes

Received 7 November 2012; accepted 20 January 2013; published online 20 February 2013
DOI: 10.1002/app.39048

INTRODUCTION

Membrane technologies have attracted broad interest from many industries and research groups. Freemantle[1] points to a significant intrinsic advantage of using membranes for gas separations relative to more conventional techniques: Membranes do not require an energy-intensive gas-to-liquid phase change in the gas mixture that is to be separated. Other cited advantages include smaller footprints and lack of mechanical complexity. The former is particularly important in environments such as offshore gas-processing platforms.

In spite of these inherent advantages, some gases, such as carbon dioxide, hydrocarbons, and water vapor can plasticize polymeric membranes and cause significant performance degradation. Koros and Fleming[2] have defined plasticization in membranes as occurring when the diffusivity of a penetrant increases significantly due to the presence of other penetrants in its neighborhood. Plasticization generally leads to a severe reduction in selectivity. In a recent review article on strategies of molecular architecture and modification of polyimide membranes for CO_2 separations,[3] Chung and coworkers add to the current wisdom of the plasticization mechanism: "Plasticization is a repertoire of pressure dependent phenomena caused by the dissolution of certain components within the polymer matrix, which disrupts chain packing and enhances inter-segmental mobility."

Glassy polymers used commonly as selective layers in thin-film composite gas separation membranes also undergo physical

Additional Supporting Information may be found in the online version of this article.

aging, the process by which these polymers in their nonequilibrium state evolve over time toward the metastable equilibrium amorphous state, thus changing physical properties such as density and permeability.[4] Thin polymer films like those used in the separation layers of composite gas separation membranes physically age orders of magnitude faster than bulk systems of the same materials.[5–12] Direct characterization of polymer thin films is, therefore, particularly relevant to the study of aging.

Perfluorocyclobutyl (PFCB) polymers are new to the membrane art, having a significant percentage of fluorine in the backbone and molecular architecture designed to increase free volume. Figure 1 shows the chemical structure of BPVE (biphenylvinylether) and 6F PFCB homopolymers. PFCB polymers typically are amorphous and exhibit exceptional processability characteristics, which enable composite membrane fabrication. Table I presents preliminary pure gas performance results of several promising PFCB polymers. Also included in Table I are entries for thin-film BPVE composite membranes prepared using two casting solution formulations. A lower concentration of BPVE in the casting solution yielded higher permeance values, suggesting a thinner selective layer.

No previous plasticization or physical aging studies have been performed on these polymers. Fundamental investigation into the plasticization and aging phenomena that occur with PFCB polymers, particularly with high partial pressure CO_2, would add to our understanding of these phenomena. To measure fundamental specific physical change data for PFCB-based composite membranes, one first needs to understand how coating conditions affect the formation of PFCB thin films. Such information also would help to explain the preliminary gas permeance findings presented in Table I. Thus, the objective of this work was to determine the thin film formation characteristics of PFCB polymer thin films to guide our development of PFCB thin-film composite membranes. In practice, the PFCB films would be coated on a nonporous or smooth microporous "gutter" layer that covers the porous support membrane. Therefore, using a nonporous model substrate is appropriate for this study. Silicon wafers were used as model substrates in this work, as they are a preferred substrate for subsequent fundamental studies that will be done on plasticization and aging. Data comparing film thicknesses on a silicon wafer (by ellipsometry) and a PFCB thin-film composite membrane (by cross-sectional TEM) for one coating condition are given in Supporting Information. The measured thickness values are the same within measurement uncertainty.

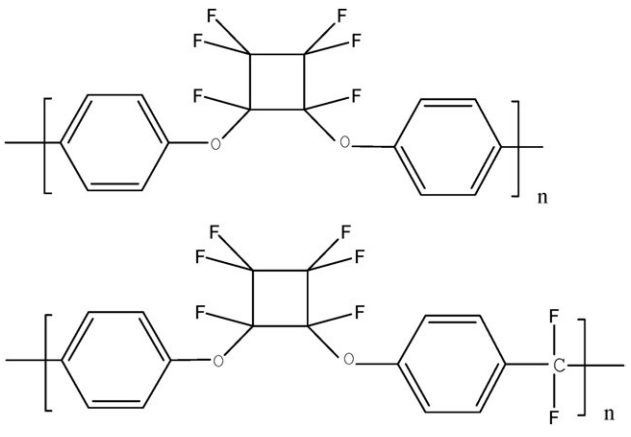

Figure 1. Chemical structures of PFCB BPVE (top) and 6F (bottom) homopolymer repeat units.

The literature describes several techniques for preparing thin-film composite membranes. Among the methods employed in laboratory research, the Langmuir Blodgett technique, spin coating, and dip-coating are preferred.[8–14] All three methods are able to control the film thickness and are easy to operate and model. Dip-coating is most similar to the method used in practice, where the thin-film selective layer is coated onto the support membrane by drawing it through a solution of polymer. Hence, we elected to form the PFCB thin films by dip-coating onto silicon wafer.

Variables studied in this work were withdrawal speed, solvent type, and concentration of polymer solution. PFCB films were characterized by measurements of thickness, refractive index, and surface morphology using ellipsometry and atomic force microscopy. The Landau–Levich equation was extended to correlate film thickness and coating conditions. Results show that polymer thickness and morphologies could be well controlled. These results are being used to guide the development of PFCB thin-film composite membranes for fundamental studies on plasticization and physical aging.

EXPERIMENTAL

Materials

These chemicals were used as received: acetone (anhydrous, 99.8%, Acros Organics), THF (anhydrous, 99.9%, Acros Organics), chloroform (anhydrous, 99.9%, Acros Organics), hydrogen peroxide (30% in water, Fisher Scientific), and sulfuric acid (≥96%, Sigma-Aldrich). Tetramer Technologies, LLC provided the biphenylvinylether-perfluorocyclobutyl (BPVE-PFCB) polymer with M_w = 110,000 Da and PDI = 1.4. Figure 1 illustrates the molecular structure of the PFCB polymer repeat unit.

Silicon wafers (Silicon Quest International) were diced into 1 × 3 cm^2 sample sizes. Prior to dip-coating studies, the silicon wafers were cleaned by sonication (VWR, B3500A-MTH) in distilled, deionized water for 15 min and then treated by immersion in a 3:1 v/v mixture of sulfuric acid and hydrogen peroxide for 1 h at 80°C. (Caution: To prepare this "Pirahna" solution, hydrogen peroxide was poured slowly into the concentrated sulfuric acid under a hood. This solution is a very strong oxidant that may react violently if mixed with organics).

PFCB Solution Preparation

PFCB solutions were prepared with concentrations of 0.25–1.00 wt % in chloroform and THF. Additional 1.00 wt % PFCB solutions were prepared in acetone. Each PFCB solution was mixed by magnetic stirrer at room temperature for 2 h before being filtered through a 0.22 μm PTFE syringe filter (Whatman).

PFCB Coating on Silicon Wafers

Clean silicon wafers were coated with PFCB solutions at 25°C using a dip-coater (Mayer Feintechnik D-3400) and withdrawal

Table I. Pure-Gas Permeation Properties of PFCB Composite Membranes to be Studied

	Pure-gas permeance (GPU)				Pure-gas selectivity		
Selective layer	N_2	O_2	CH_4	CO_2	O_2/N_2	CO_2/N_2	CO_2/CH_4
BPVE homopolymer	4.8	23	4.1	100	4.8	20.8	24.4
6F homopolymer	3.1	-	2.1	81	-	26.1	38.6
[a]1.4 wt % BPVE/chloroform	8.1	-	-	174	-	21.4	-
[a]0.3 wt % BPVE/chloroform	52.5	-	-	996	-	19.0	-

[a]Composition of casting solution used to prepare membrane.

speeds from 20 mm/min to 211 mm/min. The coated wafers were dried for 2 h at 80°C and 1700 Pa pressure immediately prior to the thickness measurements. This step was taken to ensure that all films experienced the same thermal history prior to characterization, and to avoid measurement artifacts due to physical aging.

Surface Tension Measurements

Surface tension measurements were done using a contact angle goniometer (KRÜSS GmbH, DSA10-MK2). Surface tensions of polymer solutions were measured at different PFCB concentration. DSA1v1.80 Drop Shape Analysis software (KRÜSS GmbH) was used to analyze the data using the pendant drop method. Polymer solution drops were formed inside a 10 × 10 × 47 mm^3 quartz cuvette filled with 1 mL of the corresponding solvent to saturate the vapor space and prevent evaporation of the drop. A dispensing needle with a diameter of 1.84 mm was used to form the drop, and the cuvette was covered by a Teflon lid with a 2.00 mm hole for the needle. The approximate drop volume for chloroform solutions was 10 μL and for THF solutions was 12 μL. For every measurement, the relative position of the drop to the cuvette was the same and the light source was stable to ensure consistent, high quality images for data collection. The limit line was positioned at the border between the needle and drop. Seven measurements were taken for each concentration. Average values are reported, and error bars represent ± 1 standard deviation.

Viscosity Measurements

Viscosities of PFCB polymer solutions at room temperature were measured with a cup and bulb viscometer (TA Instruments). The cup diameter was 33.8 mm, the bob diameter was 32.0 mm, the bob length was 33.5 mm, and the gap was 1.0 mm. Each solution was tested at shear rates from 100 to 1000 s^{-1} in steps of 100 s^{-1}. Tests at each shear rate were carried out for 60 s to ensure stable measurements. After completing the full set of measurements, the measurement at a shear rate of 500 s^{-1} was repeated to verify that any solvent evaporation that may have occurred did not affect the viscosity measurements. The measured data were analyzed by ARES V8.03.00 software. The reported viscosity and error bar values represent the average and standard deviation of data collected over the last 10 s at each shear rate.

Atomic Force Microscopy Images

Atomic force microscopy was employed to observe the surface morphologies and measure surface roughnesses of PFCB polymer-coated silicon wafers. Images of thin films were obtained using a Bioscope AFM (Bruker) with NanoScope III A controller. Samples were cleaned by nitrogen gas using a gas filter gun before analysis. Silicon cantilevers (MikroMasch, NSC_{15}/Si_3N_4/AIBS/50) were used as probes for the tapping mode measurements. AFM images were taken with 256 × 256 pixel resolution over areas of 10 × 10 μm at scan rate of 0.5 Hz. Root-mean-square (RMS) roughness values were calculated using NanoScope software version 6.12.

Contact Angle Measurements

Static water contact angles were measured on the surface of PFCB coated silicon wafers using a Krüss DSA10-MK2 contact angle goniometer. Deionized water was produced from distilled water that was passed through a Milli-Q water purification system (EMD-Millipore). A DI water drop (3.0 μL) was placed carefully on the sample surface. The sessile drop model was used in DSA1v1.80 drop shape analysis software to determine contact angle. For consistency, measurements were taken 1 min after each water droplet was placed on the surface. Measurements were done at minimum of three locations on each sample to get an average contact angle value with standard deviation.

Ellipsometry

Dry layer PFCB film thicknesses were measured by multiangle, single wavelength ellipsometry (Beaglehole Instruments, Picometer). The incident beam was produced by a 632.8 nm He-Ne laser source. Measurements were done at incidence angles from 56° to 80° with a step size of 4°. The reported thickness is the average of five random locations on each wafer. In this study, a PFCB-silicon dioxide-silicon substrate three layer model was applied to fit the data. PFCB thickness and refractive index based on a Cauchy model were allowed to vary and were calculated by IgorPro Software version 4.0A.

RESULTS AND DISCUSSION

Modeling

Figure 2 illustrates the process of polymer film formation. The dip-coating process forms a liquid film on the substrate. Landau and Levich[15] performed a force balance among the gravity force, surface tension, and viscous force about the meniscus region of the forming film to relate the attached, nonvolatile liquid layer thickness to the withdrawal speed. Equation (1) was proposed to estimate the thickness of the liquid layer that forms during coating with a pure, nonvolatile fluid.

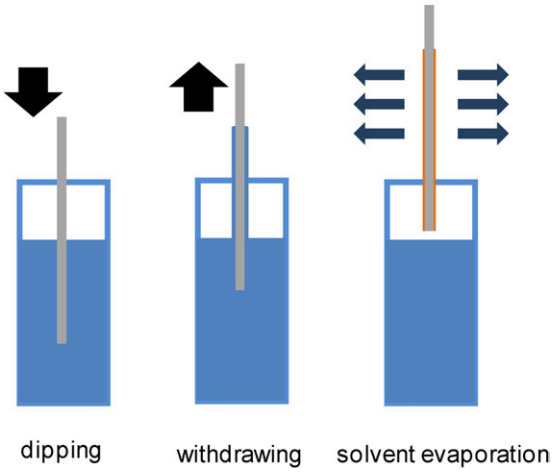

Figure 2. Schematic illustration of the polymer film formation process. [Color figure can be viewed in the online issue, which is available at wileyonlinelibrary.com.]

$$h_L = 0.94 \cdot \frac{(\eta v)^{2/3}}{\gamma_{LV}^{1/6} \cdot (\rho g)^{1/2}} \quad (1)$$

where h_L is the thickness of the liquid layer, η is the viscosity of the liquid, v is the withdrawal speed, γ_{LV} is the surface tension of the liquid, ρ is the density of the liquid, and g is the gravitational acceleration constant.

In the case of a polymer solution with a volatile solvent, solvent evaporation must be considered as the final step in the film-forming process. Since the polymer mass is conserved during solvent evaporation, dry polymer thin film thickness can be calculated using the liquid layer thickness through eq. (2):

$$h_P = h_L \cdot \frac{\rho_{\text{solution}}}{\rho_P} \cdot f_P \quad (2)$$

where h_P is the solid polymer layer thickness, ρ_P is the density of the polymer, f_P is the mass fraction of the polymer in solution, and ρ_{solution} is the density of the liquid solution, which was estimated by eq. (3):

$$\frac{1}{\rho_{\text{solution}}} = \frac{f_P}{\rho_P} + \frac{f_{\text{solvent}}}{\rho_{\text{solvent}}} \quad (3)$$

where ρ_{solvent} and f_{solvent} are the density of the solvent and the mass fraction of the solvent in solution, respectively.

Combining eqs. (1) and (2), we extended the Landau–Levich model to estimate dry layer polymer film thickness:

$$h_P = 0.94 \cdot \frac{(\eta_{\text{solution}}\, v)^{2/3}}{\gamma_{LV\ \text{solution}}^{1/6}} \cdot \left(\frac{\rho_{\text{solution}}}{g}\right)^{1/2} \cdot \frac{f_P}{\rho_P} \quad (4)$$

which can be transformed to

$$\log(h_P) = \log\left(0.94 \cdot \frac{\eta_{\text{solvent}}{}^{2/3}}{\gamma_{LV\ \text{solvent}}^{1/6}} \cdot \left(\frac{\rho_{\text{solvent}}}{g}\right)^{1/2} \cdot \frac{f_P}{\rho_P}\right) + \frac{2}{3}\log(v) \quad (5)$$

From eq. (5), if the properties of the solution do not depend significantly on withdrawal speed over the study range, then a log–log plot of polymer thickness versus withdrawal speed should have a slope value of 2/3.

PFCB Solution Viscosity

Intrinsic viscosities of PFCB polymer solutions were measured using an Ubbelohde viscometer at 25°C. Measured intrinsic viscosities, $[\eta]$, of PFCB solutions were 37.9 cm^3/g for PFCB/chloroform and 49.5 cm^3/g for PFCB/THF. Using the accepted relationship $C^* = 0.77/[\eta]$ to define the boundary between dilute and semidilute polymer solutions[16] together with solution density, overlap concentrations were estimated by eq. (6) to be 1.35 and 1.75 wt % for PFCB/chloroform and PFCB/THF, respectively.

$$C_{\text{wt}}^* = \frac{C^*}{\rho_{\text{solution}}} \quad (6)$$

Thus, the coating solutions used in this study, which range in bulk concentration from 0.25 to 1.00 wt %, all are considered to be dilute solutions.[17]

Absolute viscosities of PFCB solutions were measured using a cup and bob rheometer. PFCB/chloroform and PFCB/THF solutions exhibited slight shear thickening over the measured shear rate range (data given in Supporting Information). Shear thickening behavior of dilute polymer solutions is known to occur for dilute solutions of polymers with molecular weight higher than 1×10^5 Da in low viscosity Newtonian fluids at moderate shear rates (100 to 3000 s^{-1}).[18–20] Shear thickening may be explained by entanglement of polymer chains resulting from shear, turbulence, and Brownian motion.[21] Similar behavior has been discovered in polystyrene polymer solutions.[22] By fitting the data with a power law, $\eta = m \cdot |\xi|^{n-1}$, where ξ is the shear rate, the value for $n - 1$ for all sets of data is nearly zero, as summarized in Table II. Therefore, it is reasonable to use eq. (5) to model film thickness versus withdrawal speed data.

Refractive Index of Polymer Thin Films

Refractive index values of PFCB thin films were measured by ellipsometry using data collected at seven different angles from 56° to 80°. The reported refractive index of PFCB BPVE[23] is 1.535 at 632.8 nm for bulk films. Figure 3 shows that the refractive index of a PFCB thin film increases as the film thickness decreases below about 50 nm and becomes large when the films

Table II. Viscosity Versus Shear Rate Power Law Constants for PFCB/Chloroform and PFCB/THF Solutions

Solution	m (mPa s)	$n - 1$
1.00 wt % PFCB/chloroform	1.10	0.0003
0.50 wt % PFCB/chloroform	0.76	0.0003
0.25 wt % PFCB/chloroform	0.65	0.0003
1.00 wt % PFCB/THF	0.80	0.0003
0.50 wt % PFCB/THF	0.60	0.0003
0.25 wt % PFCB/THF	0.60	0.0002

Applied Polymer SCIENCE

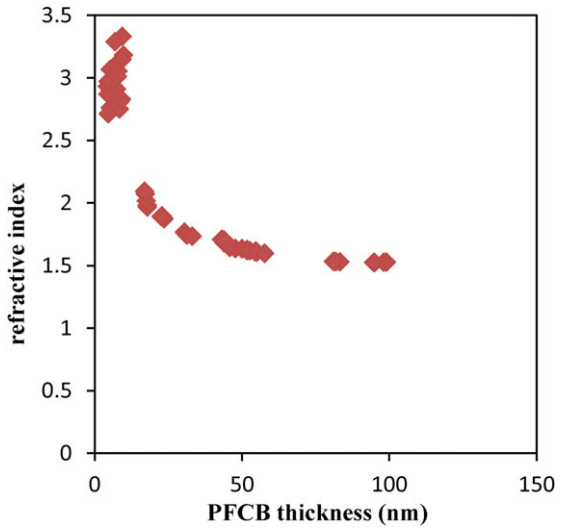

Figure 3. Refractive index of PFCB thin films measured by ellipsometry. [Color figure can be viewed in the online issue, which is available at wileyonlinelibrary.com.]

approach about 10 nm. The polymer films were prepared by coating from a PFCB/chloroform solution at different withdrawal speeds. This phenomenon is not unique to PFCB films. Such behavior has been observed in other thin film studies.[24–28] Recently, for example, Ougizawa and coworkers[24] discovered increasing refractive index with decreasing film thickness for polystyrene films and attributed this behavior to polymer densification, as described by the Lorentz-Lorenz equation:

$$\frac{n^2-1}{n^2+2}\cdot\frac{1}{\rho}=\text{constant} \tag{7}$$

They also argue that densification occurs when the concentration of precursor solution is lower than the overlapping concentration. In our case, concentrations of PFCB/chloroform and PFCB/THF solutions (0.25–1.00 wt %) are lower than their overlapping concentrations (1.35 and 1.75 wt % for PFCB/chloroform and PFCB/THF, respectively), which may cause the densification in the thin film.

For film thicknesses below 50 nm, a significant difference was found between RI values measured at the two endpoint incidence angles of 56° and 80° (data given in Supporting Information). This result indicates anisotropic properties of PFCB thin films below about 50 nm. Optical anisotropy may originate from π-stacking among the aromatic rings in PFCB, induced by interactions among these groups and silanol groups on the treated silicon wafers.[22] This interaction would cause PFCB polymer chains to tend to be aligned in a specific orientation near the polymer-surface interface. The degree of ordering is diminished moving away from the surface into the bulk film as the interactions among aromatic rings become randomized. Thus, the effect of surface-induced ordering on measured refractive index is more significant in ultrathin films, and the data for films thicker than 50 nm do not show optical anisotropy.

To account for optical anisotropy in measured film thickness values, we used multiangle ellipsometry and collected data at seven different incidence angles ranging from 56° to 80°. All seven points were used to fit PFCB thickness and refractive index based on a Cauchy model.

Effect of Withdrawal Speed and Solution Concentration on Film Thickness

Silicon wafers were selected as the coating substrates due to their high uniformity, high surface energy, and optical properties that enable PFCB film thickness to be measured accurately by ellipsometry. To ensure that the results were not affected by physical aging of the thin films, we took steps to provide the same thermal history for all samples. This included annealing the films for 2 h at 80°C, and measuring the film properties directly after this annealing step. This temperature was selected to be compatible with the support layer material that is to prepare PFCB composite membranes. Because the annealing temperature is below the intrinsic (bulk) T_g of PFCB (155°C), we also performed a control study where we measured the thickness and refractive index of PFCB thin films with similar thicknesses that were annealed for the same time period at 80 and 190°C. The thickness and refractive index measurements did not differ. This control experiment provided validation that our annealing step was sufficient to eliminate effects of physical aging on thickness and refractive index for these thin films.

Figures 4 and 5 show that PFCB film thickness increases with increasing withdrawal speed and polymer concentration in chloroform and THF solvents, respectively. Every datum point represents the average thickness among five measurement locations on one wafer. Error bars represent ± 1 standard deviation of thickness measured at the five locations. Dashed lines are results

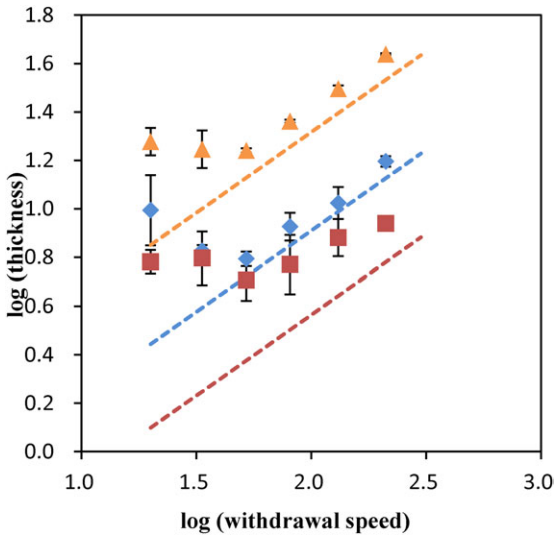

Figure 4. Role of solution concentration and withdrawal speed (in mm/min) on PFCB film thickness (in nm). Triangles, diamonds, and squares represent experimental data for 1.00, 0.50, and 0.25 wt % PFCB in PFCB/chloroform solutions. Each point represents an average of five measurements, and error bars represent ± 1 standard deviation of five measurements. Lines represent model predictions from eq. (5). [Color figure can be viewed in the online issue, which is available at wileyonlinelibrary.com.]

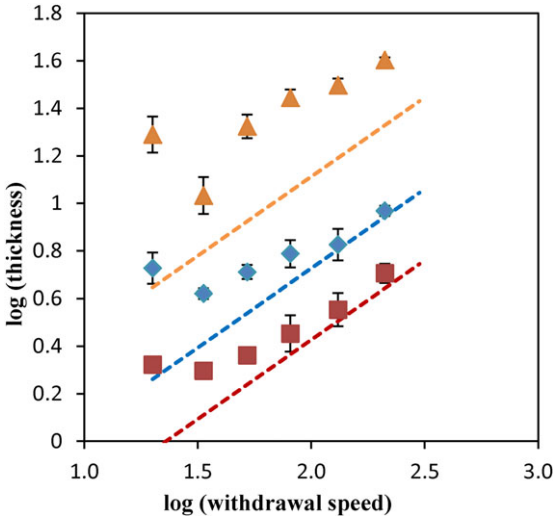

Figure 5. Role of solution concentration and withdrawal speed (in mm/min) on PFCB film thickness (in nm). Triangles, diamonds, and squares represent experimental data for 1.00, 0.50, and 0.25 wt % PFCB in PFCB/THF solutions. Each point represents an average of five measurements, and error bars represent ± 1 standard deviation of five measurements. Lines represent model predictions from eq. (5). [Color figure can be viewed in the online issue, which is available at wileyonlinelibrary.com.]

estimated from eq. (5) (the extended Landau–Levich equation). Because PFCB/chloroform and PFCB/THF solution viscosities do not depend significantly on shear rate, it is reasonable to use the extended Landau–Levich equation to predict PFCB film thicknesses. Both study systems (PFCB/chloroform and PFCB/THF) showed behavior that was expected from the extended Landau–Levich equation at higher withdrawal speeds (>50 mm/min). But at lower withdrawal speeds (<50 mm/min), we no longer observe a decrease in thickness with decreasing withdrawal speed. This deviation from theory at low withdrawal speed may be explained by the phenomenon of surface excess.

Surface excess is defined as the deviation of the surface solute (in this case PFCB polymer) concentration from its bulk concentration. It occurs when the surface tension of the solute is less than that of the solvent.[29] A high polymer concentration at the air-solution interface, relative to the concentration in the bulk solution, would yield thicker films according to eq. (4). As the wafer is withdrawn from the PFCB solution, it removes solution from the interface to form a liquid film, and depletes the surface excess of polymer. PFCB chains must diffuse from the bulk solution to replenish the surface excess, driven by the Marangoni effect. At lower withdrawal speed, more time is available for diffusion of polymer chains to the surface. The result is that the concentration of the solution removed by the silicon wafer at the air-solution interface is closer to the static (equilibrium) surface excess, which can be much higher than the bulk. At high withdrawal speed, there is less time for polymer diffusion to replenish the surface excess, and the surface concentration approaches the bulk value. Since the Landau–Levich model uses bulk concentration to estimate film thickness, it captures the experimental behavior at high enough withdrawal speeds and underestimates film thicknesses at lower withdrawal speeds.

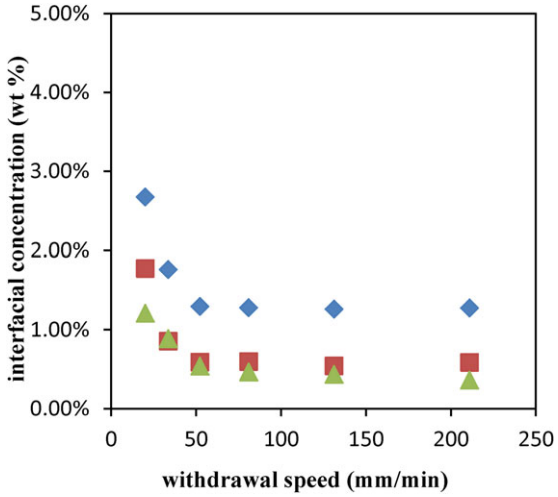

Figure 6. Estimated interfacial PFCB concentration in PFCB/chloroform at different withdrawal speeds. Diamonds, squares, and triangles represent data for 1.00, 0.50, and 0.25 wt % bulk PFCB concentration in chloroform. [Color figure can be viewed in the online issue, which is available at wileyonlinelibrary.com.]

In Figures 4 and 5, reasons for the deviation between the estimations and experimental results for 0.25 wt % chloroform solution and 1.00 wt % THF solution are not clear.

On the basis of the thickness data in Figures 4 and 5, one can estimate a theoretical interface concentration (i.e., polymer mass fraction), f_P', by eq. (8), a rearrangement of eq. (4).

$$f_P' = \frac{h_P \cdot \rho_P}{0.94} \cdot \frac{\gamma_{LV\ \mathrm{solution}}^{1/6}}{(\eta_{\mathrm{solution}}\ \nu)^{2/3}} \cdot \left(\frac{g}{\rho_{\mathrm{solution}}}\right)^{1/2} \tag{8}$$

Figures 6 and 7 present the estimated interfacial concentrations versus withdrawal speed determined from eq. (8) using

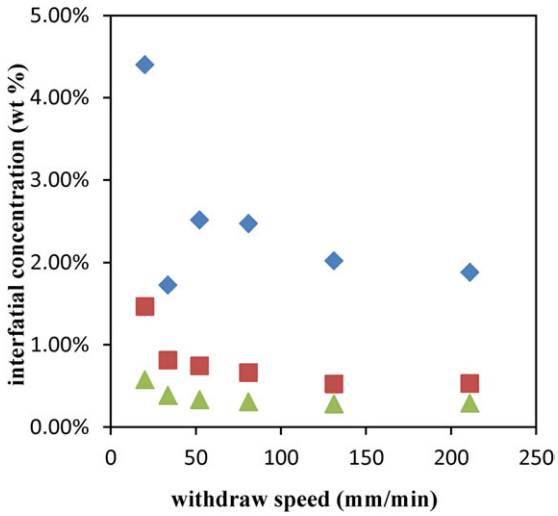

Figure 7. Estimated interfacial PFCB concentration in PFCB/THF at different withdrawal speeds. Diamonds, squares, and triangles represent data for 1.00, 0.50, and 0.25 wt % bulk PFCB concentration in THF. [Color figure can be viewed in the online issue, which is available at wileyonlinelibrary.com.]

measured thickness values from Figures 4 and 5. As the speed increases, the surface concentration gradually reaches a constant value approaching the bulk value. The estimated surface concentrations also are higher in PFCB/THF solutions. The results are consistent with work by Bloch et al.[30] who found that interfacial concentrations of polymer solutions could be orders of magnitude higher than the bulk concentration over an interfacial region with thickness in a range of tens to hundreds of Angstroms.

To determine if the estimated values from eq. (8) are reasonable, measurements of surface tension were made to allow direct calculations of PFCB surface concentrations. Figure 8 shows the relationship between surface tension and bulk PFCB concentration, presented as the molar concentration of PFCB repeat units in solutions of 0.25–10.00 wt % PFCB. The error bars represent ± 1 standard deviation among seven measurements at the same concentration. For both systems used in this study, the surface tension of the solution decreased as the concentration of PFCB increased. Ausserre et al.[31] states that a decrease of surface tension in more concentrated polymer solution indicates a surface excess. The surface excess was calculated by using the measured values of surface tension and the Gibbs adsorption isotherm,[32] given by eq. (9), where Γ is the surface excess, c is the bulk solution PFCB concentration, γ is the surface tension.

$$\left(\frac{\partial \gamma}{\partial \ln c}\right)_T = -RT\Gamma \tag{9}$$

Experimental data in Figure 8 were used to determine surface excess values, which have units of mol/m^2. To compare the results with the surface concentrations estimated in Figures 6 and 7, the surface excess needed to be converted to a wt %. The conversion was done using a layer thickness of polymer solution equal to the diameter of a PFCB repeat unit, which was estimated using Jaguar 7.7 Software (Schrödinger, LLC) at the density functional theory level. Table III summarizes other pertinent data used for the calculations.

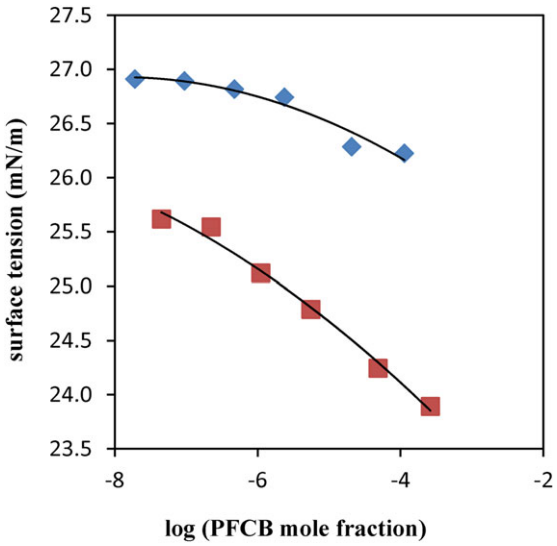

Figure 8. Surface tensions of PFCB/chloroform and PFCB/THF solutions at different concentrations. Diamonds and squares represent experimental data for PFCB solutions in chloroform and THF, and curves represent polynomial fits. Each point represents an average of seven measurements, and error bars represent ± 1 standard deviation. [Color figure can be viewed in the online issue, which is available at wileyonlinelibrary.com.]

Table III. Summary of PFCB, Chloroform, and THF Parameters

Parameter	Value
PFCB density	1.30 g/cm^3
PFCB repeat unit M_w	346 g/mole
PFCB repeat unit volume[a]	0.253 nm^3
PFCB repeat unit diameter[a]	0.8 nm
Chloroform density	1.48 g/cm^3
THF density	0.89 g/cm^3
Chloroform viscosity	0.568 mPa s
THF viscosity	0.480 mPa s
Chloroform surface tension	27.5 mN/m
THF surface tension	28.0 mN/m

[a]Estimated using Jaguar 7.7 Software (Schrödinger, LLC).

Figure 9 presents the surface concentration values in wt %. At the same bulk concentration, PFCB/THF has a higher surface excess concentration than PFCB/chloroform, which is consistent with previous estimations in Figures 6 and 7. The static (equilibrium) surface excess concentrations calculated from the Gibbs adsorption isotherm show that the surface concentrations of PFCB/chloroform and PFCB/THF solutions can be much higher than their bulk concentrations. The values also are much higher than those given in Figures 6 and 7, indicating that the values estimated from eq. (8) are physically meaningful (i.e., they fall below the equilibrium values given in Figure 9).

Typical PFCB Thin Film Morphology Characterization

Figure 10 presents surface morphology images by AFM of PFCB films with different thicknesses prepared from PFCB/chloroform

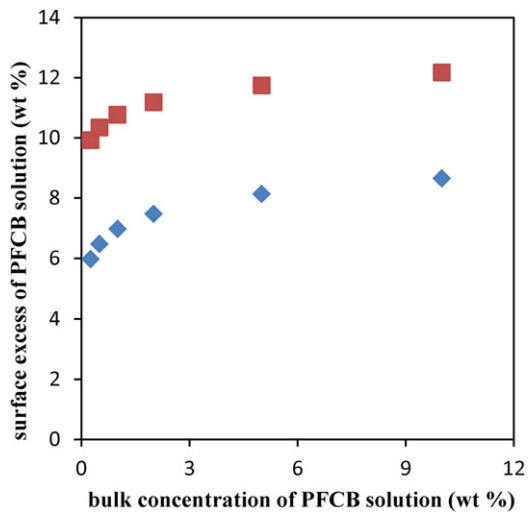

Figure 9. Surface excess concentrations of PFCB in PFCB/chloroform solutions (diamonds) and PFCB/THF solutions (squares) at different concentrations. [Color figure can be viewed in the online issue, which is available at wileyonlinelibrary.com.]

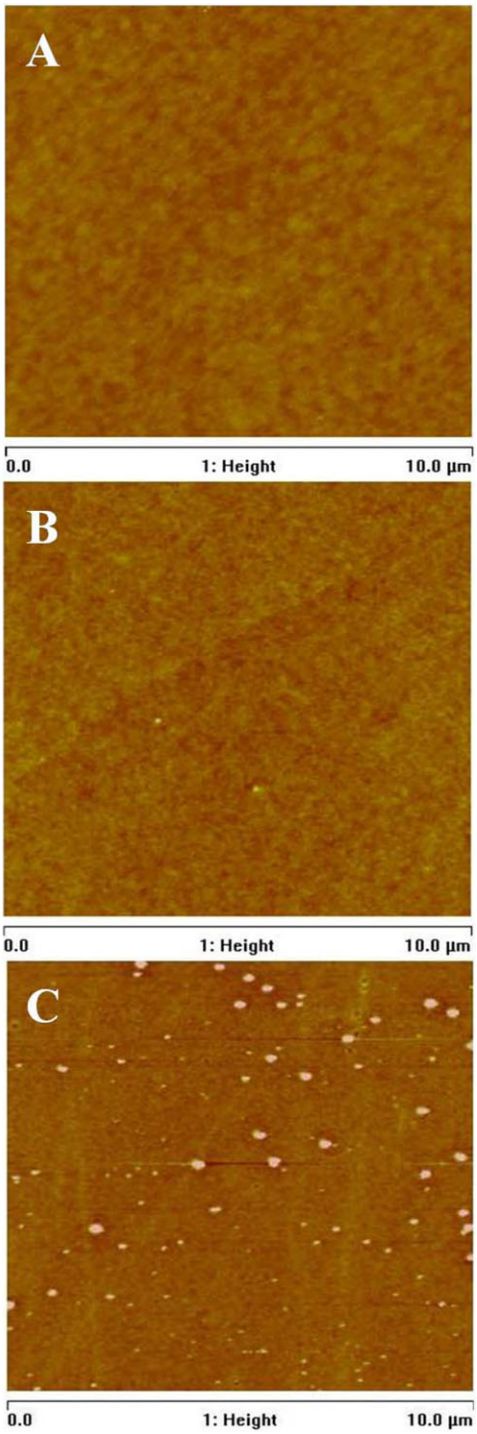

Figure 10. AFM topographical images (10 × 10 μm) of PFCB thin films on silicon substrates prepared from PFCB/chloroform solution. The *z*-scale is 10 nm. (A) 42 nm thick film, RMS roughness = 0.4 nm; (B) 26 nm thick film, RMS roughness = 1.3 nm; (C) 3 nm thick film, RMS roughness = 1.8 nm. [Color figure can be viewed in the online issue, which is available at wileyonlinelibrary.com.]

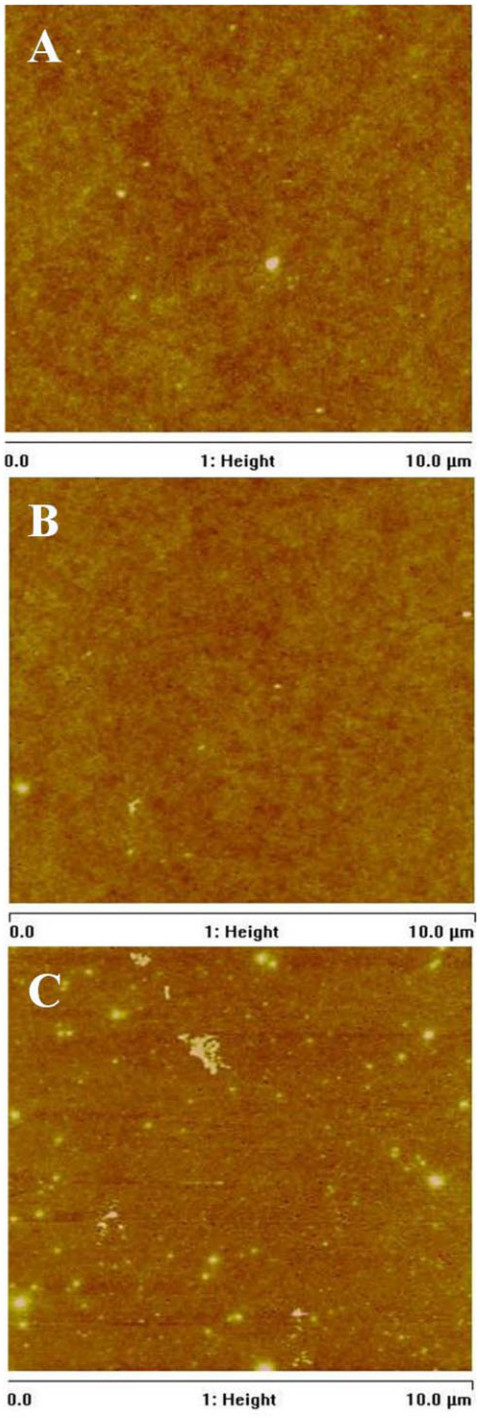

Figure 11. AFM topographical images (10 × 10 μm) of PFCB thin films on silicon substrates prepared from PFCB/THF solution. The *z*-scale is 10 nm. (A) 40 nm thick film, RMS roughness = 0.5 nm; (B) 24 nm thick film, RMS roughness = 0.6 nm; (C) 2 nm thick film, RMS roughness = 0.9 nm. [Color figure can be viewed in the online issue, which is available at wileyonlinelibrary.com.]

solution. Figure 11 presents images of films prepared from PFCB/THF solution. Three random locations on each film were scanned to get the reported average RMS surface roughness values. Generally, these films are very smooth and uniform, with RMS roughness values around 1 nm. No major defects or dewetting phenomena were observed. Table IV shows that measured water contact angles on PFCB thin films with different

Table IV. Water Contact Angle for PFCB Thin Films

Thickness (nm)	Contact angle (°)
6.3 ± 1.5	96.9 ± 0.7
9.9 ± 3.9	98.4 ± 2.1
18.9 ± 2.6	96.8 ± 2.2
21.2 ± 6.1	99.6 ± 3.3
43.3 ± 1.2	96.8 ± 2.3
52.2 ± 1.0	96.3 ± 1.8

thicknesses are the same. Together, these data and the permeance and selectivity data reported in Table I indicate that the PFCB thin films are uniform with no observed major defects.

Polymer Pattern Coated From PFCB/Acetone Solution

Unlike films prepared using chloroform and THF solvents, films prepared using acetone were not uniform. Figure 12 illustrates that different film patterns appeared at different coating conditions from 1.00 wt % PFCB/acetone solution. In Figure 12(A), the film prepared using a high withdrawing speed of 211 mm/min exhibited a rough surface with dewetted islands. Interestingly, at lower withdrawal speeds, the initial region of the silicon wafer (i.e., the first part to be coated) displayed a different film morphology than the rest of the wafer. These morphologies are shown in Figures 12(B,C). Figure 12(B) shows at 131 mm/min withdrawal speed that the film on the bottom part of the wafer is very rough; whereas, Figure 12(C) shows that the film coating the initial region of the wafer is smooth with some defects on the surface. When the film was prepared at 84 mm/min withdrawal speed, its whole surface is smooth with some defects (Figure 12D).

These different PFCB patterns might be attributed to differences in solvent-substrate interactions. Electrostatic forces, induction forces and hydrogen bonding should be considered. Treatment with Pirahna solution yields a high concentration of silanol groups on the surface of silicon wafers.[33] Both chloroform and silanol groups are good hydrogen bond donors but poor acceptors.[34] It has been shown that chloroform cannot form stable hydrogen bonds with silanol groups on silicon wafers.[35] As

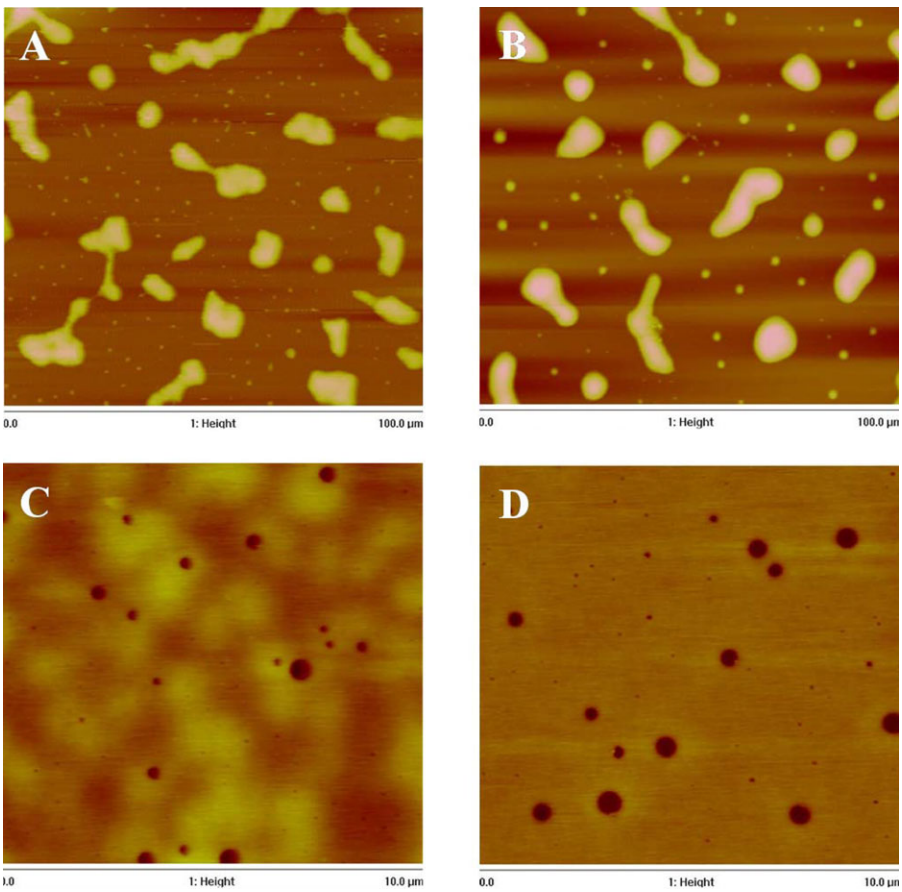

Figure 12. AFM topographical images (100 × 100 μm) of PFCB thin film on silicon substrates prepared from PFCB/acetone solution. The *z*-scale is 1 μm for A, 600 nm for B, and 50 nm for C and D. (A) Dewetting pattern of PFCB prepared from 1.00 wt % solution in acetone at withdrawal speed 211 mm/min, RMS roughness = 107.0 nm; (B) rough part of PFCB prepared from 1.00 wt % solution in acetone at withdrawal speed 131 mm/min, RMS roughness = 80.7 nm; (C) smooth part of PFCB prepared from 1.00 wt % solution in acetone at withdrawal speed 131 mm/min, RMS roughness = 2.89 nm; (D) smooth pattern of PFCB prepared from 1.00 wt % solution in acetone at withdrawal speed 84 mm/min, RMS roughness = 2.33 nm. [Color figure can be viewed in the online issue, which is available at wileyonlinelibrary.com.]

Table V. Solvent Polarizibilities and Dipole Moments

Solvent	Polarizibility × 10^{24} (cm^3)	Dipole moment (Debye)
Chloroform[34]	8.50	1.05
THF[35]	7.90	1.63
Acetone[34]	6.42	2.88

good hydrogen bond acceptors, acetone and THF do form hydrogen bonds with silanol groups. Acetone, THF, and chloroform are polar solvents, and the silanol group also is polar. Dipole–dipole interactions and induction forces can be estimated by eqs. (10) and (11),[36] where μ is dipole moment, α is polarizibility, ε_0 is permittivity of a vacuum, and r is the intermolecular distance.

$$F_{\text{dipole-dipole}} = -\frac{4\mu_i^2\mu_j^2}{(4\pi\varepsilon_o)^2 kTr^7} \tag{10}$$

$$F_{\text{induction}} = -\frac{6\alpha_i\mu_j^2}{(4\pi\varepsilon_o)^2 r^7} \tag{11}$$

Both equations are strong functions of dipole moment. Table V summarizes the dipole moments and polarizibility values of the three solvents.[36,37] The dipole moment of acetone is much larger than the values of chloroform and THF, which means acetone has much stronger dipolar and induction forces with the substrate than the other two solvents. Finally, acetone is a marginal solvent for PFCB but chloroform and THF are both good solvents. Together, these data and observations made us wonder if perhaps a depletion layer forms between silicon wafers and PFCB/acetone solution.

Fondecave and Wyart[38] discussed formation of a pure solvent depletion layer in this kind of system and proposed eq. (12) for the depletion layer thickness, e:

$$e = a_0\left(\left(\frac{A}{6\pi kT}\right)^{1/3}\varphi^{-3/4}\right) \tag{12}$$

where a_0 is the molecular size, A is the Hamaker constant, k is the Boltzmann constant, and φ is the polymer volume fraction. The Hamaker constant is usually on the order of 10^{-19} to 10^{-20} J.[39] With a PFCB concentration of 1.00 wt % in acetone, the estimated pure acetone depletion layer could be 10 nm. A depletion layer this thick would prevent the PFCB from "sensing" the underlying substrate and would lead to dewetting on the pure acetone depletion layer. After evaporation, dewetted PFCB islands would remain, as observed in Figure 12.

From eq. (12), a higher polymer concentration (volume fraction) would reduce the thickness of the depletion layer, which would make dewetting less likely. On the basis of results with chloroform and THF shown in Figures 6 and 7, lower withdrawal speed gives higher PFCB concentration in the liquid layer that coats the wafer. It is therefore reasonable to see that a smoother film surface was prepared at 84 mm/min as compared to higher withdrawal speeds. The difference in surface morphologies seen on the wafer prepared at 131 mm/min [Figure 15(B,C)] also can be explained by surface excess concentration. At the start of coating process, the concentration of polymer being coated onto the wafer is at its highest (equilibrium) value, and the depletion layer at the silicon-solution interface is thin. The result is the formation of a relatively smooth film on the initial region of the wafer. After a transient period, the surface excess is depleted, the concentration of polymer that is coated decreases, and the thickness of the depletion layer at the silicon-solution interface increases. The result is film dewetting on the bottom part of the wafer.

CONCLUSIONS

This study examined the roles of solvent, polymer concentration, and dip-coating withdrawal speed on BPVE-PFCB polymer thin film thickness and uniformity. PFCB dip-coating thickness depends on concentration and withdrawal speed, and can be estimated by an extension of the Landau–Levich equation. The accuracy of the extended Landau–Levich model for estimating layer thickness is impaired at low withdrawal speed, perhaps caused by the surface excess of PFCB polymer. PFCB films produced from solutions in chloroform and THF are highly uniform; whereas, films prepared from solutions in acetone are rough or dewetted. This behavior might be explained by formation of a surface depletion layer resulting from strong interactions between acetone and the substrate. Therefore, when selecting solvents for dip-coating, solvents that may interact strongly with the substrate are not recommended. PFCB BPVE exhibited optical anisotropy for thin films below about 50 nm thickness, likely resulting from π-stacking of aromatic groups induced by interactions among these groups and the silanol groups of the substrate. Thus, caution should be taken when using optical measurements to estimate physical properties such as density for ultrathin PFCB films on substrates that have strong interactions with aromatic groups.

This work provides guidelines for development of PFCB thin-film composite membranes. Studies are underway to characterize CO_2 plasticization and aging of PFCB composite membranes using long-term permeance measurements at different CO_2 pressures. Fundamental ellipsometry studies also are underway to characterize the swelling behavior of PFCB thin films by plasticizing gases. Results from these studies will be presented in future publications.

ACKNOWLEDGMENTS

Funding for this work was provided by the National Science Foundation under award CBET 0966581. The authors thank Meng Zhang and Sam Lukubira for assistance with viscosity measurements. They also thank Ming He for assistance with use of molecular modeling software for estimation of PFCB repeat unit dimensions.

REFERENCES

1. Freemantle, M. *Chem. Eng. News* **2005**, *83*, 49.
2. Koros, W. J.; Fleming, G. K. *J. Membr. Sci.* **1993**, *83*, 1.

3. Xiao, Y.; Low, B. T.; Hosseini, S. S.; Chung, T. S.; Paul, D. R. *Prog. Polym. Sci.* **2009**, *34*, 561.
4. Hodge, I. M. *Science* **1995**, *267*, 1945.
5. Rezac, M. E.; Pfromm, P. H.; Costello, L. M.; Koros, W. J. *Ind. Eng. Chem. Res.* **1993**, *32*, 1921.
6. McCaig, M. S.; Paul, D. R. *Polymer* **2000**, *41*, 629.
7. Madden, W. C.; Punsalan, D.; Koros, W. J. *Polymer* **2005**, *46*, 5433.
8. Huang, Y.; Paul, D. R. *Macromolecules* **2006**, *39*, 1554.
9. Kim, J. H.; Koros, W. J.; Paul, D. R. *Polymer* **2006**, *47*, 3094.
10. Kim, J. H.; Koros, W. J.; Paul, D. R. *Polymer* **2006**, *47*, 3104.
11. Kim, J. H.; Koros, W. J.; Paul, D. R. *J. Membr. Sci.* **2006**, *282*, 21.
12. Kim, J. H.; Koros, W. J.; Paul, D. R. *J. Membr. Sci.* **2006**, *282*, 32.
13. Riedl, T.; Nitsch, W.; Michel, T. *Thin Solid Films* **2000**, *379*, 240.
14. Chendake, Y. J.; Bhole, Y. S.; Lohokare, H. R.; Kharul, U. K. *Sep. Sci. Technol.* **2010**, *45*, 163.
15. Landau, L.; Levich, B. *Acta Physicochim.* **1942**, *17*, 42.
16. Graessley, W. W. *Polymer* **1980**, *21*, 258.
17. Sperling, L. H. Introduction to Physical Polymer Science, 4th ed.; Wiley: Hoboken, New Jersey, **2006**.
18. Ebagninin, K. W.; Benchabane, A.; Bekkour, K. *J. Colloid Interface Sci.* **2009**, *336*, 360.
19. Rivero, D.; Gouveia, L. M.; Muller, A. J.; Saez, A. E. *Rheol. Acta.* **2012**, *51*, 13.
20. Kamerkar, P. A.; Edwards, B. J.; Keffer, D. J.; Reneau, C. W. *Chem. Eng. Commun.* **2006**, *192*, 89.
21. Ballard, M. J.; Buscall, R.; Waite, F. A. *Polymer* **1988**, *7*, 1287.
22. Edwards, B. J.; Keffer, D. J.; Reneau, C. W. *J. Appl. Polym. Sci.* **2002**, *85*, 1714.
23. Smith, D. W.; Chen, S.; Kumar, S. M.; Ballato, J.; Topping, C.; Shah, H. V.; Foulger, S. H. *Adv. Mater.* **2002**, *14*, 1585.
24. Ata, S.; Kuboyama, K.; Ito, K.; Kobayashi, Y.; Ougizawa, T. *Polymer* **2012**, *53*, 1028.
25. Ata, S.; Muramatsu, M.; Takeda, J.; Ohaira, T.; Suzuki, R.; Ito, K.; Kobayashi, Y.; Ougizawa, T. *Polymer* **2009**, *50*, 3343.
26. Algers, J.; Suzuki, R.; Ohdaira, T.; Maurer, F. *Polymer* **2004**, *45*, 4533.
27. Kawashima, K.; Inoue, R.; Kanaya, T.; Matsuba, G.; Nishida, K.; Hino, M. *J. Phys.* **2009**, *184*, 1–4.
28. Rzodkiewicz, W.; Panas, A. *Acta. Phys. Pol. A.* **2009**, *116*, 92.
29. Mitropoulos, A.Ch. *J. Eng. Sci. Technol. Rev.* **2008**, *1*, 1.
30. Bloch, J. M.; Sansone, M.; Rondelez, F.; Peiffer, D. G.; Pincus, P.; Kim, M. W.; Eisenberger, P. M. *Phys. Rev. Lett.* **1985**, *54*, 1039.
31. Aussere, D.; Hervet, H.; Rondelez, F. *Macromolecules* **1986**, *19*, 85.
32. Reiss, H. Methods of Thermodynamics; Dover: New York, NY, **1965**.
33. Flavel, B. S.; Yu, J.; Shapter, J. G.; Quinton, J. S. *J. Mater. Chem.* **2007**, *17*, 4757.
34. Ahuja, S.; Jespersen, N. Modern Instrumental Analysis; Elsevier: Kidlington, Oxford, **2006**; *Vol. 47*.
35. Nadia, N. C.; Allen, H. C. *Chem. Phys. Lett.* **2009**, *483*, 84.
36. Prausnitz, J. M.; Lichtenthaler, R. N.; Azevedo, E. G. Molecular Thermodynamics of Fluid Phase Equilibria, 3rd ed.; Prentice-Hall: Upper Saddle River, New Jersey, **1999**.
37. Lee, J. Y.; Yun, T. S.; Santamarina, J. C. *Geochem. Geophys. Geosyst.* **2007**, *8*, 1.
38. Fondecave, R.; Brochard-Wyart, F. *Macromolecules* **1998**, *31*, 9305.
39. Ghosh, P. Colloid and Interface Science; Rajkamal Electric Press: Sonepat, Haryana, **2009**.